

A new framework for calibrating COVID-19 SEIR models with spatial-/time-varying coefficients using genetic and sliding window algorithms

Huan Zhou, Ralf Schneider

Abstract A susceptible-exposed-infected-removed (SEIR) model assumes spatial-/time-varying coefficients to model the effect of non-pharmaceutical interventions (NPIs) on the regional and temporal distribution of COVID-19 disease epidemics. A significant challenge in using such model is their fast and accurate calibration to observed data from geo-referenced hospitalized data, i.e., efficient estimation of the spatial-/time-varying parameters. In this work, a new calibration framework is proposed towards optimizing the spatial-/time-varying parameters of the SEIR model. We also devise a method for combing the overlapping sliding window technique (OSW) with a genetic algorithm (GA) calibration routine to automatically search the segmented parameter space. Parallelized GA is used to reduce the computational burden. Our framework abstracts the implementation complexity of the method away from the user. It provides high-level APIs for setting up a customized calibration system and consuming the optimized values of parameters. We evaluated the application of our method on the calibration of a spatial age-structured microsimulation model using a single objective function that comprises observed COVID-19-related ICU demand. The results reflect the effectiveness of the proposed method towards estimating the parameters in a changing environment.

1 Introduction

The susceptible-exposed-infected-removed (SEIR) [23] model has found wide application in the realm of epidemiology, mostly for quantifying the transmission dynamics of infectious diseases with incubation. The standard SEIR model assumes that the transmissibility-related parameter (denoted as μ) is time/space-invariant.

Huan Zhou
High Performance Computing Center Stuttgart (HLRS), e-mail: huan.zhou@hlrs.de

Ralf Schneider
High Performance Computing Center Stuttgart (HLRS), e-mail: ralf.schneider@hlrs.de

However, the characteristics of an epidemic (especially the recent COVID-19 pandemic) suggest that this parameter impacts the basic reproduction number R_0 and can vary, due to the season-forcing, the presence of a vaccine, the communicative connection between different regions out of the demands for the daily commute or visits and non-pharmaceutical interventions (NPIs), e.g., political measures. To better evaluate the trend of the COVID-19 pandemic, the SEIR model has consistently been extended by incorporating the time/region-varying characteristic into the parameter μ [19, 13, 12]. Therefore, estimating the values of parameter μ , i.e., calibration of these extended SEIR models to the observed data – e.g., cumulative ICU cases of COVID-19, is a crucial technical challenge that is enhanced by the time/region-varying nature of the epidemic.

The parameter μ is often deemed to be a real-valued continuous variable. This, along with its characteristic of spatial variation, easily leads to high-dimensional and broad search space. Thus, evaluating the parameter μ at a certain point in time can even be seen as a large-scale optimization problem. Naturally, expensive computation is inevitable for the practitioners to solve it. Besides, there are always communicative connections between different locations out of the demands for the daily commute or visits, i.e., parameters for different regions at certain time in point are not completely non-separable, but correlated to some extent because of the interactions between them. To this end, the values of the parameter μ for all locations (multi-dimensional parameter) should be estimated as a whole in the course of the calibration. These points prompt an important question: which optimization method we should choose to efficaciously evaluate an ensemble of values of μ in such a large-scale calibration problem? In our study, we employ Evolutionary Algorithm (EA), that can easily and efficiently be parallelized, due to the intuitive independence between individuals. In this regard, the calibration procedure has a chance to get greatly accelerated as long as the computational capacity is sufficient. Moreover, a combination of all optimized values of parameter μ during a single EA run can be obtained, since it can manage problems with non-separable interactions, which aligns with the principle of parameter interactions in the problem of our concern as well as many other real-world problems [29, 18]. There are two important EA method variants, Genetic Algorithm (GA) and Differential Evolution (DE). DE involves a direct-based mutation operator, which can better refine the solution than GA from generation to generation. Traditionally, both of them necessitate fitness evaluation of individuals after a new generation of candidates is formed. In many real-world optimization problems (including ours), the evaluation needs considerable computations; thus we attempt to constraint the number of generations (i.e. reduce the number of fitness function evaluations) for avoiding an extremely slow search process. An interesting study [28] observed that the fitness value of the best individuals drops much faster in the initial generations of GA than in DE. This observation drives us to reveal a preference for GA over DE since GA allows a good convergence within an affordable number of generations. The limited number of generations, however, speeds up the search process at the expense of degraded solution accuracy. Certainly, further measures should be taken to rule out a heavy compromise on solution accuracy. However, Parallel GAs (PGAs) are actually not frequently implemented according

to the existing studies on the application of GAs to model calibration [21, 20, 22, 10, 25, 16, 3], two of which [16, 3] used dedicated distributed GAs written in Matlab and Python. The merit of "ease-of-parallelization" fails to be fully revealed on high-performance computing clusters since Matlab and Python are not friendly to computation with high requirements for time performance. Moreover, variants of GA emerge with reinforcements with its operators, e.g. Elite GA (EGA, [16]) enhances the selection operation with elite individuals.

Not surprisingly, continuously evaluating the values of parameter μ over time is even more complex and computationally expensive. As we mentioned before, the parameter μ is time-dependent, i.e., changes regularly. If we engage in evaluating the sequence of values at one calibration execution, the number of optimized parameters a GA works with is overwhelming and induces an extremely broad search space. To enable a high probability of finding a near-optimal solution in a broad search space, the GA method demands a very high population. In this regard, more computation capacity is needed to parallelize the fitness evaluation of individuals for keeping a fast search process. However, the computation capacity is finite and not that easy to be fully obtained and reserved for a considerable time. Therefore, evaluating the sequence of values at a one-off calibration execution is not realistic. Here another question is raised: how can the problem of evaluating the values of such a spatial-/time-varying parameter be simplified? Actually, the ordered sequence of optimized values can be seen as a stream of time series data [11]; thus problem partitioning [24] makes sense in this regard. Detailedly, the set of values of parameter μ is partitioned into a number of smaller subsets so that genetic searches can be conducted for each separate partition one after another. The partial solutions of these searches are subsequently combined to obtain an estimated final solution. We need to note that there are no entirely-independent partitions in real-world problems; instead, the simulation states between the adjacent partitions are correlated in one way or another. The correlation between two adjacent partitions should thus be correctly identified (visit the `sims` data in Sect. 4.2); otherwise, the estimated final solution may not be accurate. The *sliding window* (SW) technique [6, 2] has been widely used in applications entailing the processing over data streams to perform data segmentation. This technique makes automated analysis of a large stream of data durable in such a way as to discount past data items (already being analyzed) and only consider the relevant ones in the current window. The sliding window is classified into two types: non-overlapping and overlapping [8]. The overlapping sliding window (OSW) is characterized by two parameters – `opt_window_size` and `opt_shift_size`. The former denotes the window size and the latter signifies the shift/overlapping size, which should be less than the given window size. The non-overlapping sliding window (NOSW) can thus be seen as a special overlapping one, where the shift size is 0.

This article aims to develop a compute-based implementation of framework/-tool based on a novel calibration method/algorithm combining the *single-objective* parallel EGA and OSW for the SEIR models extended with time/spatial-varying parameters. Given the feasibility of running our calibration method within acceptable computation time, we implement it in Fortran programming language [9] that

is extensively used in numerical and scientific computing since it can be highly optimized to run on high-performance computers, and in general the language is suited to producing parallel code (e.g., parallel EGA) where performance is important. Our calibration method also uses the OSW technique to divide the complex problem into overlapping sub-problems embracing different partitions. To increase the calibration accuracy, it incorporates *directional information* that aids in dynamically refining the ranges in which the values of parameter μ are allowed to vary and then guides the search space of the next partition in the direction of convergence, as the window slides forward. We further propose a framework/tool attached with input/output modules in which the user can flexibly insert their data source, SW-related and GA-related parameters, and consume the ultimate solution containing a set of near-optimal values of the parameter. In this way, the implementation of the method is treated as a black box, which is abstracted by our framework away from the user. The problem inherent in the OSW-based calibration implementation is that the solution at a certain point in time cannot be tuned again at a later time once it is determined, even if it is not satisfactory [2]. It can be addressed by imposing a post-tuning operation, i.e., subsequent improvement of the incorrect solution with a GA operation. Therefore, our calibration framework supports two types of calibration events: automated calibration and *one-off calibration*. The automated calibration is supposed to adjust in accordance with directional knowledge and automates over a given period of time without any empirical interference from the user side. On the other hand, the one-off calibration enables post-tuning of the undesirable solution by performing a GA operation at given points in time.

In the next section, we describe an extended SEIR model used to test our proposed calibration algorithm. Sect. 3 describes the general methodology for the calibration algorithm. In Sect. 4 we then introduce the structure of the calibration framework used for the optimization and demonstrate the utility of the framework to calibrate the extended SEIR Model for representing the hospitalization dynamics related to COVID-19 disease in Germany. We show the results comparing the simulated dynamics and observed data in Sect. 5. Finally, we conclude in Sect. 6.

2 CoSMic model

The model chosen for testing our calibration method is an extended SEIR model, which is proposed in a recent research study [19]. This extended model specifically takes sub-national/spatial and temporal variation in ICU-relevant disease dynamics into account. It is also called an SEIR-based age-structured spatially-disaggregated microsimulation model, which is hereafter abbreviated as *CosMic*. CosMic is designed and run for simulating and forecasting COVID-19-related ICU demand at the state level.

A crucial technical challenge in applying it is its accurate calibration against observed data, e.g., the daily number of ICU patients with COVID-19, at the sub-regional/NUTS-2 regions, as the history of the disease strongly affects predictions of

future system behavior. Specifically, the calibrated CoSMic represents a near-optimal estimation of the (floating-point) parameter $R0_effects/\mu$ that impacts the reproduction number R_0 . The values of parameter μ vary and depend on miscellaneous factors – seasonal change, location, pharmaceutical- and political-interventions, among others. I.e., the parameter μ varies as the time lapses and the region changes. The rest of this paper uses the $R0_effects$ and μ interchangeably.

There are altogether 38 NUTS-2 regions across Germany and initially the values of μ range from 0.1 to 0.9. The reported ICU case data set was extracted from the novel German intensive care register database established in March 2020 by the German Interdisciplinary Association for Intensive Care and Emergency Medicine (DIVI), since the real-life implementation is anticipated.

3 Methods

In our study, we applied the Genetic Algorithm (GA) to the calibration of our CoSMic model by using the sliding window technique. Therefore, before getting into the details of the calibration method, the concept and structure of the sliding window technique and GA are briefly introduced and their representation in the CoSMic model is illustrated as well.

3.1 Overlapping sliding window

We let notation

$$U = \langle \vec{\mu}_1, \vec{\mu}_2, \vec{\mu}_3, \dots, \vec{\mu}_N \rangle \quad (1)$$

be an ordered stream of *regular time series* data [11], which consists of data points over N time steps/weeks. Each data point is represented as a vector used for storing a sequence of optimized values of our targeted parameter μ for different regions at a given time instant. These data points are not measured independently, but with *one-way dependence*, meaning that the estimated value of data point $\vec{\mu}_x$ in CoSMic strongly depends on the model state expressed by its predecessor $\vec{\mu}_{x-1}$, not vice versa. This is due to that the observed data, to which our model CoSMic is calibrated, is relevant to the COVID-19 patients admitted to the ICU. *ICU-ill* is an intermediate state in the CoSMic model [19] and thus the number of current patients with ICU-ill state is estimated based on that of the earlier ones with other states (such as susceptible, exposed and infected). Theoretically, optimizing U at a single calibration execution is the simplest way to get a complete solution since we do not need to explicitly store any model state during calibration. However, it is unrealistically computationally expensive. Therefore, the SW technique is applied to perform the problem partition [24]. Individual calibrations are then conducted for solving segmented problems one after another. Consequently, the solution of every

single problem combines to determine the best search trajectory of the spatial-/time-varying parameter μ .

The SW is proven to be efficacious in tackling optimization problems where the parameters of a model might vary over time [1, 26]. This technique considers only the active data items in the current window that nicely complies with the principle of one-way dependence. With the same window size, segmenting using OSWs is almost twice longer than that using NOSWs. Likewise, the estimation time on the data encompassed by OSWs is thus almost two times longer compared to the NOSWs. We demonstrate a bias in favor of OSWs, notwithstanding such an increase in size and computation. This is due to that OSW enables a more correct approximation by allowing for the application of additional knowledge to further refine some of the active data items in the precedent window (see Sect. 4.3). Naturally, the two parameters – `opt_window_size` and `opt_shift_size` are key factors affecting the approximation performance (i.e., accuracy) of the proposed calibration method. We tried varied values for them in this study, and the combination of 4 and 1 resulted in the best performance. Fig. 1 exemplifies the application of the OSW-based segmentation to segment the calibration procedure from t -th week to $(t + 5)$ -th week.

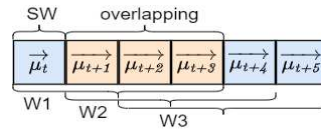


Fig. 1 The schematic of segmentation and overlapping sliding overlapping window

3.2 Genetic algorithm

Genetic algorithms (GAs) [17] are population-based metaheuristics based on evolutionary processes of natural systems, which were invented by John Holland [27] in 1960s; hereafter they are extensively studied and developed by Goldberg [14] and De Jong [7], among others. Basically, GAs are used to find global near-optimal solutions to optimization and search problems by iteratively applying evolution concepts including selection, mating, mutation and "survival of the fittest". The calculation of fitness value is done by executing the defined fitness function. A simply-implemented GA first initializes a random-based population comprising a set of individuals/*chromosomes*, and then evaluates the fitness for each individual. After that, it selects the parent having the strongest fitness, followed by crossover, and mutation operations to work out a new population. Finally, it calculates the fitness of each new individual and selects the next generation. This process is repeated until any of the predefined termination criteria is met. Hereafter the terms individual and chromosome are used interchangeably.

3.2.1 Representation

The first step in utilizing GAs for a particular problem is to design an appropriate representation of chromosome. In this study, our targeted optimization problem (i.e., CoSMic) concerns the evaluation of parameter μ at the level of 38 NUTS-2 regions over time. The best experimental values of `opt_window_size` and `opt_shift_size` are 4 and 1, respectively, and the μ is a real-valued continuous variable; thus the chromosome is coded in the form of a vector of 38×4 floating point numbers/*genes* [15], as shown in Fig. 2.

The regions of interest are numbered in ascending order starting from 1 up to 38. Each gene μ_i^s alters the basic reproduction number R_0 and is calibrated so that our model results for regions s at COVID-19 week point t can best reproduce the corresponding observed data. All the genes in the same week comprise a subset and then all these disjoint subsets $\langle \vec{\mu}_t, \vec{\mu}_{t+1}, \vec{\mu}_{t+2}, \vec{\mu}_{t+3} \rangle$ form the solution to the listed sub-problem constrained by the span of the current window. Initially, each gene takes value in a predefined interval $[0.1, 0.9]$, which is problem-dependent and thus provided by the input parameter file. The structure of chromosome representation remains unchanged as the sliding window moves; but we change to a new sub-problem embracing different optimized targets. Their values are subject to updated lower and upper bounds, which are determined according to the model results at the previous week.

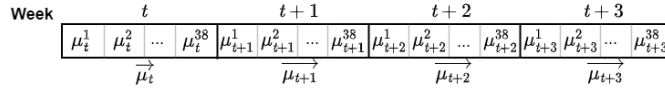


Fig. 2 Chromosome representation of a candidate solution within certain time window

Our representation scheme can be directly passed to the objective function (see Equation 3) without any intermediate encoding or decoding steps. Further, the genetic operators (mutation and crossover) are accordingly defined to handle floating-point numbers (refer to Sect. 3.2.3).

3.2.2 The objective function and fitness function

Aside from fixing a proper representation, the user must specify the objectives for initiating GA. Our targeted CoSMic model produces a critical simulation output – per-day ICU data, against which the model is calibrated. The per-day ICU (hospitalization) data can intrinsically reflect the epidemic dynamics because of their reliability. Thus a time slice mathematical representation of the CoSMic model is as follows:

$$CoSMic(\langle \vec{\mu}_t, \vec{\mu}_{t+1}, \vec{\mu}_{t+2}, \vec{\mu}_{t+3} \rangle) = \overline{ICU}^{sim}, \quad (2)$$

where the vector $\langle \vec{\mu}_t, \vec{\mu}_{t+1}, \vec{\mu}_{t+2}, \vec{\mu}_{t+3} \rangle$ is the parameters to be calibrated, and the vector \vec{ICU}^{sim} is the simulated ICU cases.

Essentially, the parameter calibration of the above time slice CoSMic model means adjusting the values of parameters that can make the ICU data match the observed one in the course of t -th to $(t+3)$ -th week closely. There are a set of closeness indicators used to evaluate the goodness-of-fit of the calibration but we have used only root mean square error (RMSE [5]) for our study. A smaller value of RMSE indicates a set of parameters introducing a closer approximation to the observed data. Therefore, we formulate our objective function as follows:

$$Obj = \sqrt{\sum_{i=1}^m \sum_{j=1}^n (ICU_{i,j}^{obs} - ICU_{i,j}^{sim})^2 / (m * n)}, \quad (3)$$

where in this study "m=28" indicates the 28-day window and "n=38" represents the number of regions. The $ICU_{i,j}^{obs}$ and $ICU_{i,j}^{sim}$ are the observed and simulated ICU cases on the j th region at i -th day of the predefined time window, respectively. In the search process of GA, the individuals with higher fitness values (i.e., smaller RMSE) are more likely to survive. Therefore, the fitness function is further created by simply applying a negative to the above objective function:

$$Fitness = -Obj \quad (4)$$

3.2.3 Implementation/Structure of proposed GA heuristic

We apply Elite GA (EGA) so as not to lose the few best-found solutions. It improves "simple" GA in a way that passes elite individuals (i.e., individuals with the largest fitness values) on to the next generation without crossover and mutation operations, unless new individuals with larger fitness are generated and selected as the new elite individuals (the maximum number of elite individuals applied was 5 in this study). The main steps involved in our implementation of EGA can be summarized as follows:

1. **Initialization:** construct N candidate solutions to form an initial population. The initial population constitutes base solutions for successive generations. Each candidate solution (chromosome) is generated randomly and the values of its genes are chosen by obeying a uniform distribution between the given lower and upper bounds.
2. **Fitness evaluation:** calculate the fitness value for each individual in the population according to the fitness function expressed in Equation 4. Then all the individuals are sorted in ascending order of the fitness values. The individuals with higher fitness values are thus regarded as fitter candidate solutions.
3. **Elitism:** select individuals with the largest fitness values as the elite individuals, which will be straightforwardly passed on to the next generation without crossover and mutation operations.

4. The following steps are repeated until there are N individuals in the population of the next generation.
 - 4.1. **Selection:** select good candidate solutions as parents to reproduce the next generation of the population. There are different strategies for selection but here we have used only roulette wheel selection [7]. The idea of roulette wheel selection is to assign a probability value to each chromosome based on its fitness value, and then select two chromosomes as the parents according to the probability distribution. The chromosomes having the higher fitness value have a better chance to be selected; thus a chromosome could repeatedly be selected.
 - 4.2. **Crossover/Recombination:** in order to generate offspring solutions, a crossover operator is applied to the selected parents with the given crossover probability (80% for our experiment). The proposed algorithm uses a whole arithmetic crossover strategy, which is useful with floating-point solutions. It takes a percentage of each parent gene and adds them to produce new solutions (two children). The value of the percentage is randomly generated. The newly produced children are inserted into the population of the next generation.
 - 4.3. **Mutation:** mutation enhances diversity at a smaller probability value (10% for our experiment). We have used a simple procedure where we randomly choose one gene from a chromosome and change its value randomly.
5. Repeat steps 2-4 until termination criteria are satisfied. In our study, the algorithm stops when the maximum number-of-generations or the convergence-of-population is achieved. Finally, the best-found solution is presented.

The Fortran version of our calibration framework has been developed based on the above-described EGA. The values of algorithm-related parameters need to be specified beforehand (visit the input module in Fig. 3) to define a specific heuristic search.

4 Proposed framework

In this section, we introduce the new framework¹ for calibrating SEIR models extended with the characteristic of time-/spatial-variation (like CoSMic). This framework encapsulates our calibration algorithmic details of integrating the GAs and OSW as core component. Besides, our framework provides input and output components, where the user group can flexibly insert the configurable parameters and consume the optimized solution.

¹ <https://github.com/hpcralf/CoSMic>

4.1 High-level structure

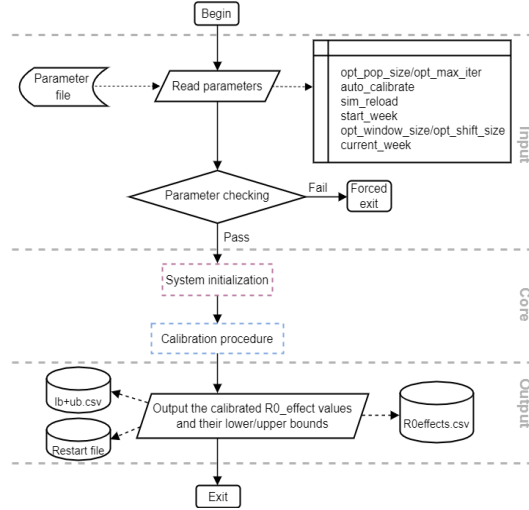


Fig. 3 The synthetic workflow of the proposed calibration framework

Fig. 3 demonstrates a high-level (abstract-level) overview of our calibration framework structure mainly consisting of three sub-components: *a*) input, *b*) core, and *c*) output. The input component reads all the needed parameters from a `static.parameter.dat` file and prepares them for initializing the framework. The input validation is called for the detection of unauthorized input before it is passed on to the following components. It is applied on the semantic level – enforces the correctness of the parameters’ values in the context of CosMic use case. The input parameters fall into three different categories: *a*) automation-relevant, *b*) system, and *c*) GA-relevant/control. In detail, the automation-relevant parameters target the data segmentation and then the automation procedure that is performed by the SW technique. They can be enumerated as follows: 1) `auto_calibrate`: a logical value indicating an automated (TURE) or a one-off calibration procedure (FALSE), 2) `opt_window_size`: window size, 3) `opt_shift_size`: shift factor, 4) `current_week`: the window stops sliding when `current_week` reaches, and 5) `start_week`: the start point of the first window. The system parameter here is `sim_reload`, which is a logical value indicating a restart file reload (TURE) or not (FALSE). The timescales of `opt_window_size` and `opt_shift_size` are expressed in weeks. In the beginning, the values of parameter `start_week` and `sim_reload` are respectively assigned 1 and FALSE, which indicate the initial state of our automatic calibration event. The GA-relevant parameters are featured by the following control and range-related indexes: 1) `opt_pop_size`: population size, 2) `opt_max_size`: number of generations, 3) `opt_lb`: the lower bound of the parameter, and 4) `opt_ub`: the upper bound of the parameter.

System initialization and calibration procedure comprise our core component. They contain a level of steps that combine to perform a relatively complicated routine and thus are unfolded separately in Sections 4.2 and 4.3. In the end, the best solution (optimized values of parameter μ from `start_week` to `current_week`) is written to an output file `R0effects.csv`, which is ready to be accessed in the further. The directional information indicating the upper and lower bounds of the parameter μ for the next round calibration is recorded into an output file `lb+ub.csv`. Besides, the relevant restart file, from which the next calibration event starts, is outputted.

4.2 System initialization

Fig. 4 dissects the system initialization component with a sequence of initializing actions. The observed/referred ICU cases are summed by regions (either state or NUTS-2) and then organized in chronological order. And then `sim_switch` of the derived (`struct`) data type is initialized before it is passed and analyzed in the simulation module. Its member `sim_reuse` is initialized with `FALSE` implying that the involved simulation starts from scratch or reloads a restart file. Once the window starts to slide forward, the `sim_reuse` is changed to `TRUE` meaning that the simulation receives the passed `sims` data, which is understood as the previous model state and perceived as the new starting point. The other members will be introduced on demand in the future. When the simulation entails a reload of a restart file (with `sim_reload` as `true`), the specific `start_week` is provided to indicate from which week this simulation starts. Accordingly, the starting evaluated date represented by this simulation should be adjusted by adding `start_week` to the seed date (March 9, 2020), i.e., the first day in week 1 of the German COVID-19 epidemic.

4.3 Calibration algorithm

The workflow of the calibration procedure is shown in Fig. 5, from which we can obviously observe that the calibration procedure goes in two distinct directions in terms of `auto_calibrate`. The disabled `auto_calibrate` indicates a one-off calibration which is more like a static post-tune of the unsatisfied values by applying a GA. The `start_window` and `end_window` are directly parsed from the parameter `opt_names`. On the contrary, in the course of automated calibration, the initial `start_window` and `end_window` are determined to include the observed starting date, and thus the initial window size is not necessarily identical to the predefined `opt_window_size`. The above sequence of steps is reduced to preprocessing. The parallel routines – GA and automated calibration – come immediately after the preprocessing. Next, we move to the details of automated calibration, on which we will focus in this Section.

Algorithm 1 Pseudo-Fortran code for solving automated calibration with OSW and GA for certain NUTS-2 region

```

1: function AUTOMATED_CALI( $R0\_effects$ ,  $start\_window$ ,  $current\_window$ ,  $opt\_window\_size$ ,
   $opt\_shift\_factor$ ,  $sims$ ,  $Obs\_ICU$ ,  $opt\_lb$ ,  $opt\_ub$ )
2:   while  $start\_window \leq current\_window$  do
3:     Generate initial population  $\vec{P}$ 
4:      $end\_window \leftarrow start\_window + opt\_window\_size - 1$ 
5:     if  $end\_window > current\_window$  then
6:        $end\_window \leftarrow current\_window$ 
7:     end if
8:     repeat
9:        $R0\_effects(start\_window:end\_window, :) \leftarrow \vec{P}$ 
10:       $\overrightarrow{Fitness} \leftarrow FITNESS\_CAL(R0\_effects, start\_window, end\_window, sims, sim\_switch,$ 
       $Obs\_ICU)$ 
11:      Selection enhanced with elitism, crossover, mutation in terms of  $\overrightarrow{Fitness}$ 
12:      Update  $\vec{P}$ 
13:      until Stopping criteria reached
14:       $R0\_effects(start\_window:end\_window, 0) \leftarrow$  Best chromosome in  $\vec{P}$ 
15:      ADJUST_LBUB( $R0\_effects(start\_window:end\_window, 0)$ ,  $sims$ ,  $sim\_switch$ ,  $Obs\_ICU$ ,
       $opt\_lb$ ,  $opt\_ub$ )  $\triangleright$  Adjust  $opt\_lb$  and  $opt\_ub$  in terms of the fitness value
16:      CoSMIC( $R0\_effects(start\_window:end\_window - (opt\_window\_size - opt\_shift\_size), 0)$ ,
       $sims$ ,  $sim\_switch$ )  $\triangleright$  Record the sims data at week of
       $end\_window - (opt\_window\_size - opt\_shift\_size)$ 
17:       $sim\_backup \leftarrow sims$ 
18:       $sim\_switch\%sim\_reuse \leftarrow .TRUE$ 
19:       $sim\_switch\%sim\_reload \leftarrow .FALSE$ 
20:       $start\_window \leftarrow start\_window + opt\_shift\_size$ 
21:       $end\_window \leftarrow end\_window + opt\_shift\_size$ 
22:      if  $end\_window > current\_window$  then
23:         $end\_window \leftarrow current\_window$   $\triangleright$  Slide the window by  $opt\_shift\_size$ 
24:      end if
25:    end while
26:    return  $R0\_effects(:, 0)$ 
27:    Record the updated  $opt\_lb$  and  $opt\_ub$ 
28:    Write the recorded sims data to a restart file
29: end function
30: function FITNESS_CAL( $R0\_effects$ ,  $start\_window$ ,  $end\_window$ ,  $sims$ ,  $sim\_switch$ ,  $Obs\_ICU$ )
31:    $\overrightarrow{Eva\_ICU} \leftarrow$  CoSMIC( $R0\_effects(start\_window:end\_window, :)$ ,  $sims$ ,  $sim\_switch$ )
32:    $\overrightarrow{Fitness} \leftarrow RMSE(\overrightarrow{Eva\_ICU}, Obs\_ICU)$ 
33:   return  $\overrightarrow{Fitness}$ 
34: end function
35: procedure ADJUST_LBUB( $R0\_effects$ ,  $start\_window$ ,  $end\_window$ ,  $sims$ ,  $sim\_switch$ ,  $Obs\_ICU$ ,
   $opt\_lb$ ,  $opt\_ub$ )
36:    $Eva\_ICU \leftarrow$  CoSMIC( $R0\_effects(start\_window:end\_window, 0)$ ,  $sims$ ,  $sim\_switch$ )
37:   ( $diff, correct\_coeff$ )  $\leftarrow$  ADJUST_STRATEGY( $Eva\_ICU$ ,  $Obs\_ICU$ )  $\triangleright$   $diff \leftarrow$  Eval_ICU(last day
  of  $end\_window$ ) -  $Obs\_ICU$ (last day of  $end\_window$ )
38:   if  $diff.lt. 0$  then  $\triangleright$  Lower than the observed data
39:      $opt\_lb \leftarrow avg\_R0$   $\triangleright$   $avg\_R0 \leftarrow$  mean( $R0\_effects(start\_window:end\_window, 0)$ )
40:      $opt\_ub \leftarrow \min(avg\_R0 + correct\_coeff, 0.9)$ 
41:   else if  $diff.gt. 0$  then  $\triangleright$  Higher than the observed data
42:      $opt\_lb \leftarrow \max(avg\_R0 - correct\_coeff, 0.1)$ 
43:      $opt\_ub \leftarrow avg\_R0$ 
44:   else
45:      $opt\_lb \leftarrow \max(avg\_R0 - correct\_coeff, 0.1)$ 
46:      $opt\_ub \leftarrow \min(avg\_R0 + correct\_coeff, 0.9)$ 
47:   end if
48: end procedure

```

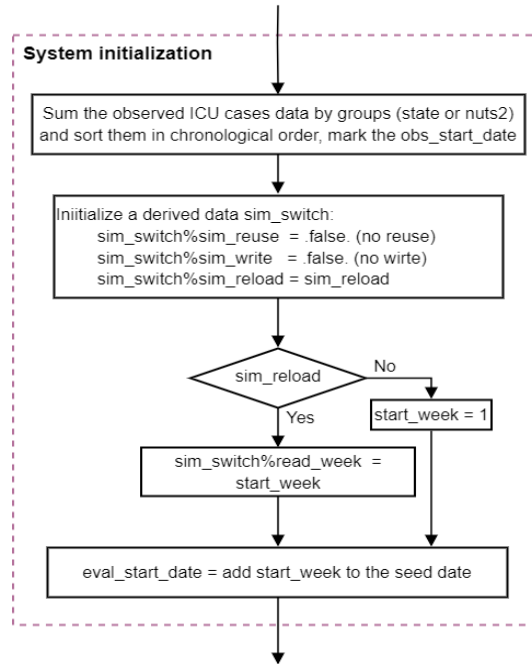


Fig. 4 The workflow of system initialization component

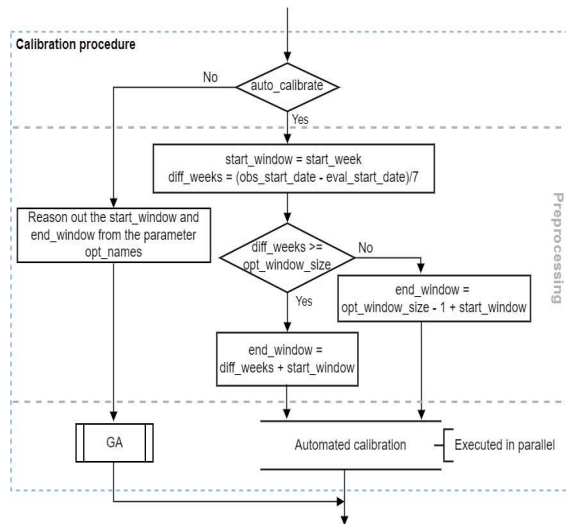


Fig. 5 The workflow of calibration procedure component

Algorithm 1 explains in detail the automated calibration procedure (for a given NUTS-2 region), where there is a two-tier nested loop. In Line 10, the fitness values for individuals can be evaluated independently in parallel. In our experiment, we use the master-slave parallelism for the EGA [4]. The inner repeat-until

loop is entailed by the GA subroutine; the outer `while` one accomplishes the automation procedure by moving forward the sliding window, until the predefined `current_window` reaches. The automation firstly goes through a GA subroutine, which starts from an initial population and then iteratively optimizes the `R0_effects` from week `start_window` to `end_window` until the stopping criteria (see Line 13) are satisfied. In this GA subroutine, we evaluate the fitness value (as shown in Lines 30-34) by calculating the root-mean-square error (RMSE), which represents the differences between the ICU cases estimated by CoSMic simulation and those observed between `start_window` and `end_window`. This is followed by the sequence of selection enhanced with elitism, crossover and mutation. The selection is conducted in the principle of working out a new population from (fitter) individuals with higher fitness values.

After escaping from the GA loop, we call the simulation twice with the so far best-found solution (i.e., chromosome with the highest fitness value in \vec{P}) to prepare for the next calibration period. The preparation is twofold: 1) One is to dynamically adjust the lower and upper bounds of the `R0_effects` value (refer to the procedure `Adjust_lbub` represented by Lines 35-48) based on directional information mentioned in Sect. 1. The adjustment strategy is thus to some extent problem-specific but in principle should enable self-heuristic search space as the window slides. In our case, the directional information combines the current solution (see Line 39) and the difference between observed and evaluated ICU cases at the most recent point in time of the current window (see Line 37). The former can prevent the estimated μ from fluctuating strongly over adjacent periods and yields good performance with low RMSE. The latter is justified by the approximately three-week delay between exposure to SARS-CoV-2 and hospitalization due to COVID-19. 2) The other is to memorize the `sims` data (i.e., simulation status) on the first day of a certain week from which the next calibration period starts (see Line 16). Next, we activate the `sim_reuse`, slide the window by `opt_shift_size` and move to the next period if the start point of the current window does not exceed the `current_week`. In this regard, the called CoSMic simulation will use the passed `sims` data as its initial state after the first calibration period. After escaping from the outer loop, the recorded `sims` data will be permanently written to a restart file which can be reloaded during the subsequent calibration procedures. Such strong `sims` data dependence will cause error propagation temporally. The occurrence of dramatic drops/rises (peak/nadir) during the observed ICU data series could further deteriorate the error propagation. To alleviate it, a smoothing mechanism can be integrated to retouch the already-calibrated parameter values.

5 Results

Our use case – CoSMic model – considered week-by-week variations in our time-varying parameter μ , the first task is thus to determine the values of two critical OSW-related parameters – `opt_shift_size` and `opt_window_size`, which define

how a series of optimized parameters should be split and then correlated. The calibration results may deviate from the observed data when the assumed `opt_shift_size` is longer than the timescale of actual variation. We can recall that the best-combined values of `opt_window_size` and `opt_shift_size` are 4 and 1, by revisiting the Sect. 3.1. Table 1 demonstrates the production setup (i.e., values of critical parameters) for the calibration procedure across the NUTS-2 regions from March 9th 2020 (i.e., COVID-19 week 1) to August 2nd 2022 (i.e., COVID-19 week 125). The sample size we choose is the full German population. The CoSMic model is stochastic and executed 40 times for each window (time period) and then the estimated ICU cases are averaged across the multiple outputs in order to reduce variance in parameter estimation and obtain a stable trend for it.

Table 1 Calibration parameters and values

Simulation parameters	Values
Sample size	83237124
Iteration numbers	40
Calibrated weeks	COVID-19 week1-week125
Calibrated regions	All 38 German NUTS-2 regions

Our framework allows real-time calibration; thus we aim to obtain decent solutions within reasonable execution time by assuming a limited number of iterations and population size. Table 2 provides a layout of the GA user-defined configuration file used for calibrating the model parameters. We can observe that the generation number is set as 10, since the fitness value level off as the iteration goes. The population size is 80, which is large enough to guarantee diversity. A crossover probability of 0.9 and a mutation probability of 0.1 are used in this simulation. The upper and lower limit of the parameter μ for CoSMic model is read from the input files. Each chromosome is represented as a parameter array that comprises 4×38 (i.e., 152) floating point numbers in their own range, given that there are altogether 38 NUTS-2 regions across Germany.

Table 2 GA parameters and values

GA parameters	Values
Population size	80
Generation number	10
Mutation probability	0.1
Crossover probability	0.8
Mutation method	Uniform Random
Selection type	Linear scaling
Crossover type	Logical arithmetic
Elitism	5
Chromosome size	152 floating point numbers

The CoSMic model is not a hypothetical example, where the true optimum set of parameter values was known by assumption. We cannot use this to examine whether our calibration method is capable of finding the optimum. Therefore the accuracy of our calibration method was then studied by checking with the data fitting, i.e., the difference (RMSE) between the model-estimated ICU dynamics and the observed one. Next, we will show how our framework performs in calibration accuracy and speed under the production setup (see Table 1) and the given GA-related parameters (see Table 2). As we mentioned in Sect. 3.2.1, initially the GA search range of μ is set to $[0.1, 0.9]$. Among all the 38 regions in Germany, Berlin, Stuttgart and Trier are typical of regions with low, medium and high density, respectively. Fig. 6 plots the comparison curves in the three regions for our single objective (i.e., to minimize the average RMSE between the model-estimated ICU dynamics and the observed data). A high match between the estimated average and observed ICU cases can be obviously observed in Berlin and Stuttgart regions and the important overall patterns (e.g., uphills, downhills, etc.) can consistently be captured in a satisfactory way. The average RMSE is in the order of 12 over all the NUTS-2 regions and the past two years, which is low given that most values of our dataset are larger than 100, and indicates a good calibration accuracy.

We ran the above calibration procedure (refer to Table 1) on the NEC cluster (aka. Vulcan) located at HLRS. Vulcan consists of multiple nodes of different types. The compute node type we used is Intel Haswell E5-2660v3. Each of the Haswell compute node has 20 cores running at 2.6 GHz with 128 GB DDR3 main memory. The applied GNU compiler version was 11.2.0 and the version of OpenMPI/4.1.2 was run. In this experiment, 80 parallel nodes are requested and a single MPI process is launched per node. Each MPI process further spawns 20 OpenMP threads that concurrently execute the 40 CoSMic model runs for each generation. Owing to the parallelized implementation, this calibration procedure took approximately 1.5 days to complete.

6 Conclusion

We explore a calibration method to fit an extended SEIR model of COVID-19 to location-specific ICU data for estimating spatial-/time-varying parameters. This calibration method combines the OSW technique and EGA to achieve satisfactory estimation accuracy within a reasonable time. On the one hand, the applied OSW technique is used to segment a given calibration procedure into multiple ones over shorter time slices; thus it enables an automated process of parameter estimation by moving forward the window. On the other hand, the EGA is an improved global optimization method in high-dimensional spaces and is applied to each segmented calibration. Naturally, it is simple to be parallelized in code and becomes highly effective by simultaneously calculating the fitness values of multiple individuals when executed in parallel. Besides, we use a high-performance computing environment to foster many GA heuristic search processes in parallel, allowing us to effectively

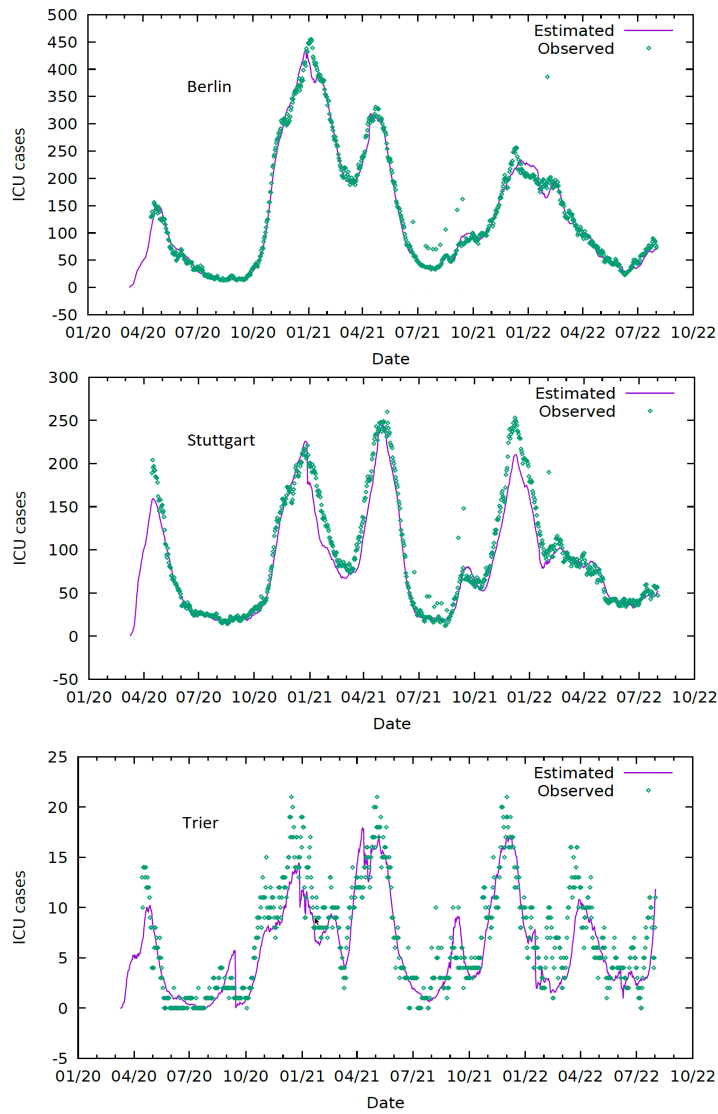


Fig. 6 Model-fitting of weekly transmission coefficient μ and daily hospitalizations in regions of Berlin, Stuttgart and Trier.

explore a broad parameter space in a time-efficient manner. Further, the implementation details of this algorithm are wrapped in our calibration framework and thus hidden from the user. Our framework offers the input/output components, where the user can insert the calibration and EGA settings of interest and consume the ultimate solutions at his/her convenience as well. Overall, our calibration framework shows promise for estimating spatial-/time-varying parameters and working with the models with different settings. In the future, we envision that the works include *a)* strengthen the validation of our calibration algorithm by comparing it with the existing calibration algorithms, *b)* accelerate the optimization speed, and *c)* improve the optimization accuracy.

Acknowledgements We would like to acknowledge the funding provided by the BMBF & MWK Baden Württemberg through the work package "generic scenarios and prototypical implementations" (AP2) in the project CIRCE (under Grant no. 16HPC062).

References

1. Akhavizadegan, F., Ansarifard, J., Wang, L., Huber, I., Archontoulis, S.V.: A time-dependent parameter estimation framework for crop modeling. *Scientific reports* **11**(1), 1–15 (2021)
2. Babcock, B., Datar, M., Motwani, R., O’Callaghan, L.: Sliding window computations over data streams. Tech. rep., Stanford InfoLab (2002)
3. Barnhart, B.L., Sawicz, K.A., Ficklin, D.L., Whittaker, G.W.: Moesha: A genetic algorithm for automatic calibration and estimation of parameter uncertainty and sensitivity of hydrologic models. *Transactions of the ASABE* **60**(4), 1259–1269 (2017)
4. Cantú-Paz, E., et al.: A survey of parallel genetic algorithms. *Calculateurs paralleles, reseaux et systems repartis* **10**(2), 141–171 (1998)
5. Chai, T., Draxler, R.R.: Root mean square error (rmse) or mean absolute error (mae)?—arguments against avoiding rmse in the literature. *Geoscientific model development* **7**(3), 1247–1250 (2014)
6. Datar, M., Gionis, A., Indyk, P., Motwani, R.: Maintaining stream statistics over sliding windows. *SIAM journal on computing* **31**(6), 1794–1813 (2002)
7. De Jong, K.A.: An analysis of the behavior of a class of genetic adaptive systems. University of Michigan (1975)
8. Dehghani, A., Sarbishei, O., Glatard, T., Shihab, E.: A quantitative comparison of overlapping and non-overlapping sliding windows for human activity recognition using inertial sensors. *Sensors* **19**(22), 5026 (2019)
9. Documents, F.S.: <https://gcc.gnu.org/wiki/GFortranStandards>
10. Dolan, H., Rastelli, R.: A model-based approach to assess epidemic risk. *Statistics in bio-sciences* **14**(3), 452–484 (2022)
11. Esling, P., Agon, C.: Time-series data mining. *ACM Computing Surveys (CSUR)* **45**(1), 1–34 (2012)
12. Girardi, P., Gaetan, C.: An seir model with time-varying coefficients for analyzing the sars-cov-2 epidemic. *Risk Analysis* **43**(1), 144–155 (2023)
13. Gleeson, J.P., Brendan Murphy, T., O’Brien, J.D., Friel, N., Bargary, N., O’Sullivan, D.J.: Calibrating covid-19 susceptible-exposed-infected-removed models with time-varying effective contact rates. *Philosophical Transactions of the Royal Society A* **380**(2214), 20210120 (2022)
14. Goldberg, D.E.: Zen and the art of genetic algorithms. In: *Proceedings of the 3rd international conference on genetic algorithms*, pp. 80–85 (1989)

15. Golub, M.: An implementation of binary and floating point chromosome representation in genetic algorithm. In: Proceedings of the 18th International Conference on Information Technology Interfaces, pp. 417–422 (1996)
16. Guo, D., Olesen, J.E., Pullens, J.W., Guo, C., Ma, X.: Calibrating aquacrop model using genetic algorithm with multi-objective functions applying different weight factors. *Agronomy Journal* **113**(2), 1420–1438 (2021)
17. Holland, J.H.: Genetic algorithms. *Scientific american* **267**(1), 66–73 (1992)
18. Iorio, A.W., Li, X.: Incorporating directional information within a differential evolution algorithm for multi-objective optimization. In: Proceedings of the 8th annual conference on Genetic and evolutionary computation, pp. 691–698 (2006)
19. Klüsener, S., Schneider, R., Rosenbaum-Feldbrügge, M., Dudel, C., Loichinger, E., Sander, N., Backhaus, A., Del Fava, E., Esins, J., Fischer, M., et al.: Forecasting intensive care unit demand during the covid-19 pandemic: A spatial age-structured microsimulation model. *medRxiv* (2020)
20. Leardi, R.: Genetic algorithms in chemometrics and chemistry: a review. *Journal of Chemometrics: A Journal of the Chemometrics Society* **15**(7), 559–569 (2001)
21. Leardi, R.: Nature-inspired methods in chemometrics: genetic algorithms and artificial neural networks. Elsevier (2003)
22. Leardi, R.: Genetic algorithms in chemistry. *Journal of Chromatography A* **1158**(1-2), 226–233 (2007)
23. Li, M.Y., Muldowney, J.S.: Global stability for the seir model in epidemiology. *Mathematical biosciences* **125**(2), 155–164 (1995)
24. Lucasius, C.B., Kateman, G.: Understanding and using genetic algorithms part 2. representation, configuration and hybridization. *Chemometrics and Intelligent Laboratory Systems* **25**(2), 99–145 (1994)
25. Monteiro, L.H.A., Gandini, D., Schimit, P.H.: The influence of immune individuals in disease spread evaluated by cellular automaton and genetic algorithm. *Computer methods and programs in biomedicine* **196**, 105707 (2020)
26. Ratnavale, S., Hepp, C., Doerry, E., Mihaljevic, J.R.: A sliding window approach to optimize the time-varying parameters of a spatially-explicit and stochastic model of covid-19. *PLOS Global Public Health* **2**(9), e0001058 (2022)
27. Sampson, J.R.: Adaptation in natural and artificial systems (john h. holland) (1976)
28. Santos Amorim, E.P.d., Xavier, C.R., Campos, R.S., Santos, R.W.d.: Comparison between genetic algorithms and differential evolution for solving the history matching problem. In: International Conference on Computational Science and Its Applications, pp. 635–648. Springer (2012)
29. Yu, X., Gen, M.: Introduction to evolutionary algorithms. Springer Science & Business Media (2010)